

Extended-range computation of Wannier-like functions in amorphous semiconductors

Uwe Stephan* and Richard M. Martin

Department of Physics, University of Illinois at Urbana-Champaign, Urbana, Illinois 61801

David A. Drabold

Department of Physics and Astronomy, Ohio University, Athens, Ohio 45701-2979

(Received 10 December 1999)

We have computed first-principles occupied Wannier-like functions within an unprecedented spatial range in a realistic model of amorphous Si containing 4096 atoms. To avoid the computation of eigenstates we applied the $O(N)$ Fermi-operator expansion method. The functions decay exponentially in space in a fashion similar to the best-localized occupied Wannier states in crystalline silicon. While their decay lengths do not depend on the local distortions, the functions have an intricate nonspherical structure depending on the disorder in the material.

Since the 1930s it has been known that electron states in crystals can be expressed in either an extended (Bloch) form or a localized (Wannier) form.¹ The long-range decay of the Wannier functions (WF's) is qualitatively different for metals and insulators, and the exponential localization in the latter case is the basis of the fundamental theory of the insulating state developed by Kohn and others² and the modern theory of polarization.³ Moreover, the nature of the localized functions plays a key role in the new $O(N)$ electronic-structure computational schemes which scale only linearly with the number of atoms in the system,⁴ and in efficient methods for incorporation of electron correlation in insulators.⁵

The importance of (orthonormal) WF's is based on two principal properties. First, since they are unitary transformations of the canonical eigenstates of a given one-particle Hamiltonian, these functions span the same space as the eigenstates. Second, the freedom in the choice of this transformation allows one to select those WF's which are to a maximum extent localized. In particular, if one computes localized WF's which are created from all occupied eigenstates, one gets functions which reflect the bonding properties of a given system.

While the computation of WF's in molecules (localized molecular orbitals) has a long history in quantum chemistry (cf. Ref. 6), there have only been few computations of such functions in solid-state physics.⁵⁻⁹ When starting from Bloch eigenstates, these computations adopted a certain choice of the Bloch phase factors.⁷ However, the requirement of maximum localization of WF's makes the unitary transformation unique, provided a certain localization criterion has been selected. Such maximally localized WF's have recently been computed by Marzari and Vanderbilt.⁶ The explicit computation of WF's from eigenstates is only feasible, however, for systems which are not too large because the computation of a complete band of eigenstates scales with the third power of the system size. On the other hand, the investigation of the exact localization behavior of these functions requires their computation over longer spatial distances. This localization behavior is still the topic of some debate, primarily for two reasons. First, there have been proofs for a number of special

systems that exponentially localized WF's exist, if these states are computed from energy bands which are separated from other bands by finite energy gaps.^{10,11} This suggests the existence of exponentially localized occupied WF's in insulators. There has not yet been a general proof of this statement, however. Second, the dependence of the exponential decay length of the WF's (or the related density matrix) on the gap width is still under discussion.^{4,10-13} This is caused by the fact that the dependence of occupied WF's on the energetic position of the unoccupied states can only be an indirect one mediated by the properties of the Hamiltonian. Moreover, in disordered systems the localized WF's cannot depend, in general, on either the global gap between the highest occupied and lowest unoccupied eigenstates (HOMO-LUMO gap) nor some sort of local gap formed by any locally relevant localized (defect) eigenstates.^{14,15}

In this paper, we present direct extended-range computations of occupied WF's in a realistic 4096-atom model of *a*-Si (Ref. 16) using an approximate density functional method. We avoided the computation of eigenstates by applying the linear-scaling Fermi-operator expansion (or projection) method^{9,17} with a subsequent approximate orthonormalization of the projected states. Our generalization of this method to nonorthonormal basis states and the $O(N)$ implementation of the orthonormalization have been described in detail in Ref. 9. The advantage of this scheme is that the effort of performing the projections scales linearly also with the number of atoms in the localization regions, and thus allows us to use quite large regions. To further increase the accuracy of our method, these regions were dynamically adjusted within the orthonormalization.

In Ref. 9, we had already presented preliminary results for WF's in diamond and amorphous carbon cells containing 512 atoms and using a simple LDA-based tight-binding-like Hamiltonian. The Hamiltonian of the present paper is the fully first-principle local-orbital LDA Hamiltonian of Sankey and Niklewski.¹⁸ The atomic orbitals in this Hamiltonian are strictly set to zero outside a certain cutoff range (5.0 bohr radii for Si). With this Hamiltonian, the Fermi energy of the given system was computed using the dynamic projection method described in Ref. 19. The number of Chebychev

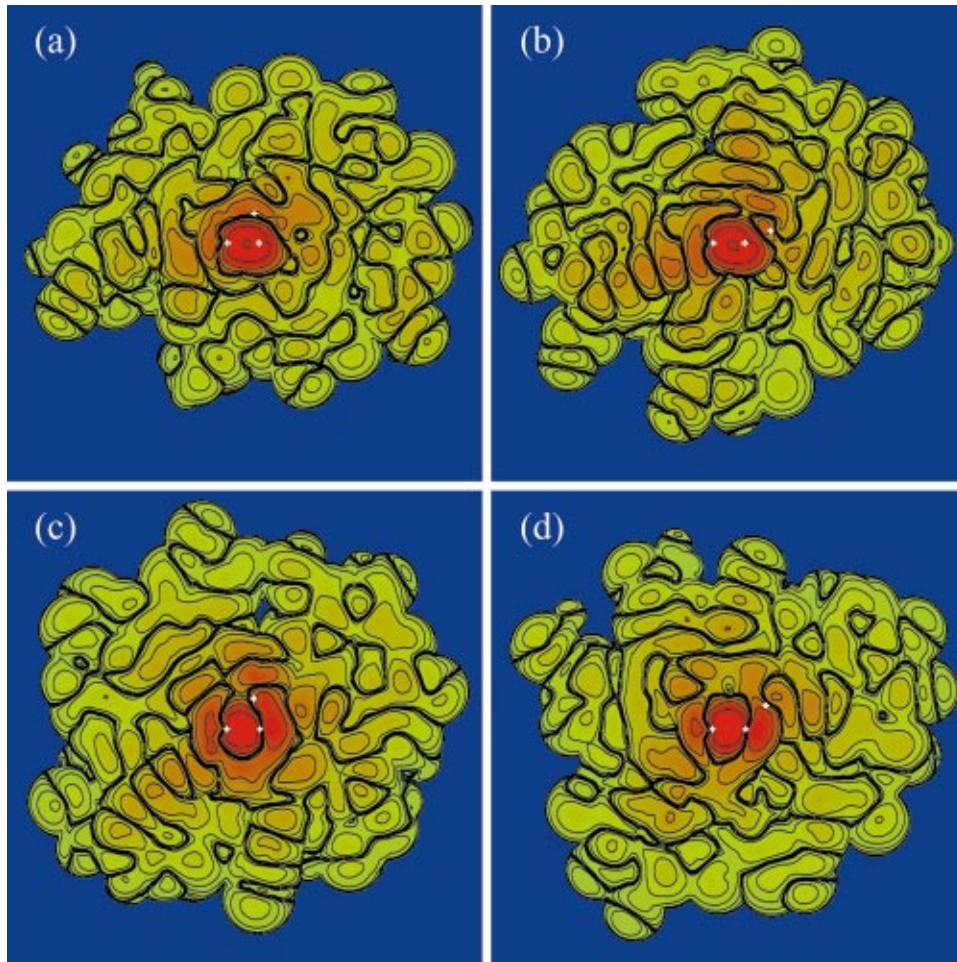


FIG. 1. (Color) Charge-density plots with isodensity contour lines for two truncated and orthonormalized Wannier-like functions within planes in a 4096-atom *a*-Si model. The upper two panels depict one WF in two different planes while the lower two panels show another function in two planes. The colors have been mapped to the logarithms of the charge density stretching over about 20 orders of magnitude from its maximum value (red) through green to the minimum finite value (blue). The deepest blue is assigned to zero charge density outside the localization regions. The small white crosses indicate the positions of the atoms defining the plane.

polynomials needed to get convergence in this computation (130 for $\beta=80$) was then used throughout the scheme.

Because of the complete fourfold coordination of the system, we could start with bonding orbitals as initial functions

which are bonding combinations of hybrid orbitals pointing in bond directions.^{6,9,20} The localization regions used during the projections then contained all atoms within seven bond steps from the originating bond.

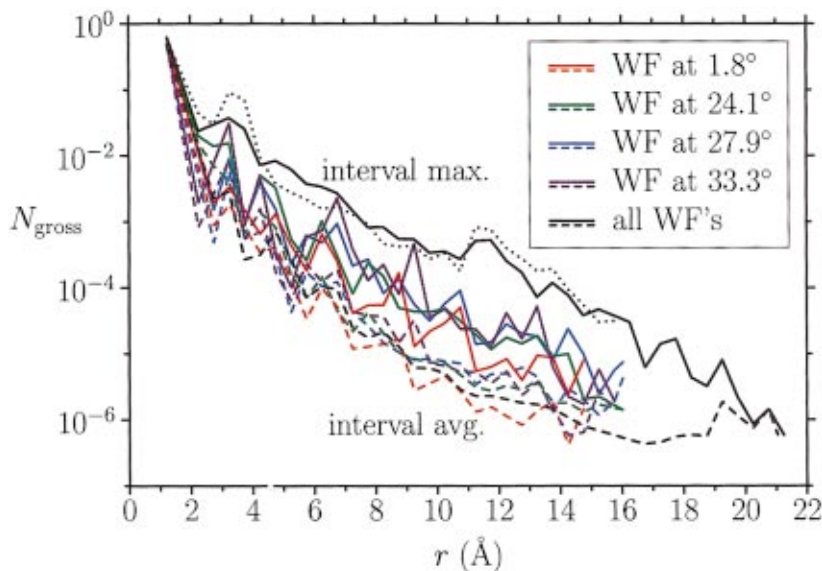


FIG. 2. (Color) Mulliken's atomic gross populations vs distance from bond center for four WF's in the 4096-atom *a*-Si model. Solid (dashed) lines, maximum (average) population values in distance intervals of 0.5 Å; black lines, population values for all WF's. The WF's are centered at bonds that are attached to atoms with the specified standard deviations of the bond angles. The WF's at the atoms with deviations of 24.1° and 27.9° are the functions plotted in Figs. 1(c), 1(d) and 1(a), 1(b), respectively. The dotted line gives the maximum population values for all WF's before orthonormalization.

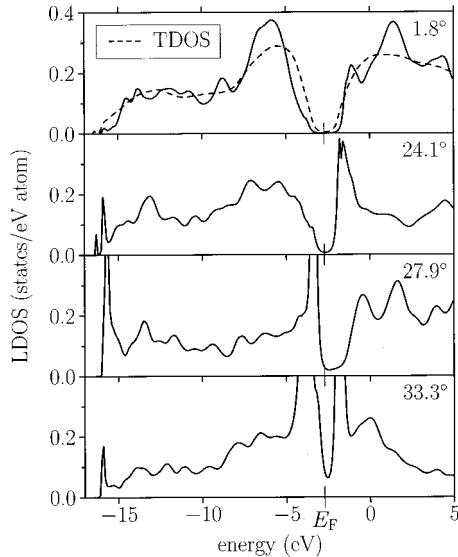


FIG. 3. Local densities of states at the atoms selected in Fig. 2 with the specified standard deviations of the bond angles. The dashed line in the upper panel represents the total density of states in the 4096-atom *a*-Si model.

As an example, Fig. 1 shows the charge densities within planes for two selected orthonormalized projected WF's in the *a*-Si model. The planes are defined by three atoms which are indicated by small white crosses in the figures. Two of these atoms form the originating bond of the WF, while the third atom is a neighboring atom of this bond. The function plotted in the top panels of Fig. 1 is located at a bond which is situated at one of the most distorted atoms in the whole system. The three atoms in Fig. 1(a) form a bond angle of 83° only, while the bond angle in Fig. 1(b) amounts to 155° . The bottom panels in Fig. 1 depict two planes through another WF where the bond angles are 79° [Fig. 1(c)] and 130° [Fig. 1(d)], respectively. The standard deviations of all bond angles at these atoms are 27.9° for the upper and 24.1° for the lower panels. After the dynamic orthonormalization, the localization regions contained 476 atoms in the upper case, and 441 atoms in the lower case. The colors describe a logarithmic charge density plot with densities reaching from its maximum value as shown in red (≈ 10 electrons/ \AA^3) through green and blue (blue for zero density outside the localization regions). The minimum finite charge density plotted was about 10^{-19} electrons/ \AA^3 . Additionally, the figure contains contour lines of equal charge density where the density logarithm crosses an integer value. The thick black lines which are composed of many contour lines represent node lines at which the WF changes sign.

As can be seen in Fig. 1, the large local distortions at the selected atoms result in a sizable asymmetry of the WF's already in the immediate vicinity of the central bond. Nevertheless, the functions are clearly localized and bonding at the originating bond, and are antibonding to the neighboring atom to fulfil the orthogonality constraint. When going out further in space, the functions become highly irregular due to the disordered nature of the system. The WF's oscillate several times until they reach the boundary of the localization regions. These boundaries are sharp in the logarithmic plots due to the cutoff in the atomic orbitals. As a further interest-

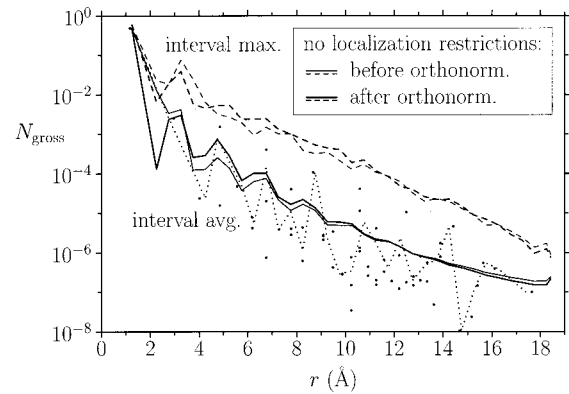


FIG. 4. Mulliken's atomic gross populations vs distance from bond center for all projected WF's without localization restrictions in a 512-atom *a*-Si model. Thin (thick) lines, before (after) orthonormalization; dashed (solid) lines, maximum (average) population values within distance intervals of 0.5 \AA . The figure also contains the population values at the exact atomic positions (thick dots) and the interval averages (dotted line) for the orthonormalized WF's in a crystalline 512-atom Si cell.

ing feature, the resulting WF's show a clear tendency to become nonspherical. This is a result we had already found earlier using a simpler Hamiltonian.⁹ The functions prefer to spread out in certain bond directions while they decay more quickly in other parts of their environment. In some cases, as in Fig. 1(a), the overall function may be better described by an ellipsoidal shape instead of a spherical one.

To better quantify the radial decay of our localized WF's, Fig. 2 depicts the decay of Mulliken's atomic gross populations of the WF's of Fig. 1 (green and blue lines) along with another two WF's within distance intervals of 0.5 \AA . The additional WF's are attached at the atom with the largest standard deviation (33.3°) of the bond angles found in the whole system (purple lines), and between atoms with the small deviations of 1.8° and 11.6° (red lines). The solid lines depict the maximum population values in the given distance intervals which are an indication of the envelope functions of the WF's. The dashed lines represent the average population for all atoms within these intervals. Furthermore, the black lines specify the maximum and average population values for all orthonormalized WF's in the same intervals.

First, the radial structure of the WF's corresponding to certain neighbor shells is also visible in this figure. Nevertheless, the overall radial decay of the envelope functions is approximately exponential. In particular, the decay of all WF's plotted in Fig. 2 appears to be very similar. The average population values, on the other hand, show a saturation for larger distances from the bond centers. This flattening of the decay comes from the fact that the average values have to approach the maximum values for farther distance intervals which contain only a few atoms. However, these average values indicate that also the WF's at the majority of less distorted atoms have essentially the same decay behavior as the WF's shown in Fig. 2. The decays, therefore, are similar despite the fact that the atoms in this system are characterized by very different local densities of states (LDOS) due to different local distortions. In Fig. 3 we have plotted the LDOS (computed with the recursion method²¹) at four atoms selected in Fig. 2. While the LDOS at the tetrahedral-like

atom with standard deviation of 1.8° possesses a quite large gap, this gap is filled to different extents at the other three atoms (corresponding to different local weights of the eigenstates of the system). Hence, the decay of the WF's in an amorphous system appears to be independent of the structure of the gap within the related LDOS.

Figure 2 (dotted line) also shows that the orthonormalization of the WF's does not noticeably change the exponential decay of these functions. This is confirmed by corresponding computations in a smaller 512-atom *a*-Si model where we could compute WF's without imposing LOC restrictions (Fig. 4). However, it has been known for a long time²² that nonorthogonal WF's can be better localized. The orthonormalization in our case indeed moves some charge from the central region of the WF to the next neighbor shells. The overall exponential decay, however, is not influenced by the orthonormalization. This result follows from the nature of the orthonormalization process as discussed by Kohn and Onffroy.¹⁴

Furthermore in Fig. 4, the thick dots depict the population values of the unrestricted and orthonormalized projected states at the exact atomic positions in a crystalline 512-atom Si cell. Comparing the envelope as well as interval averages for this and the amorphous cell, we see that the exponential decay of the WF's in the crystalline and amorphous systems appears to be similar although defects reduce the HOMO-LUMO gap in the *a*-Si model.²³ This also confirms our dis-

cussion above on the gap dependence of WF's. In disordered systems, the decay of the WF's may be related not to HOMO-LUMO gaps, but to the separation of the occupied and unoccupied *extended* states, i.e., the width of the mobility gap. This mobility gap is expected to be quite similar in crystalline and amorphous Si.²³

We remark that for this smaller model, the exactly determinable relative error in the band-structure energy for our WF's computed with the $O(N)$ functional of Mauri and Ordejón²⁴ was 8×10^{-5} without and 6×10^{-4} with localization regions.

In summarizing, using the linear-scaling Fermi-operator expansion method we have computed first-principle occupied WF's with long tails in a huge model of an amorphous tetrahedrally coordinated semiconductor (*a*-Si). These computations allowed us to study the radial structure and decay of these functions for distances up to about seven bond steps from the central bond. The WF's have a complicated nodal structure and decay approximately exponentially. This exponential decay appears to be independent of the width of local energy gaps and is similar in crystalline and amorphous Si cells.

This work was supported by DARPA Contract No. DABT63-94-C-055 and DOE Grant No. DEFG02-96-ER45439. D.A.D. acknowledges financial support from NSF Contract No. DMR 96-18789.

*Present address: Fachbereich 6, Theoretische Physik, Universität-GH Paderborn, 33098 Paderborn, Germany.

¹G. Wannier, Phys. Rev. **52**, 191 (1937).

²W. Kohn, Phys. Rev. **133**, A171 (1964); R. Resta and S. Sorella, Phys. Rev. Lett. **82**, 370 (1999).

³D. Vanderbilt and R.D. King-Smith, Phys. Rev. B **48**, 4442 (1993); R.W. Nunes and D. Vanderbilt, Phys. Rev. Lett. **73**, 712 (1994); R. Resta, Rev. Mod. Phys. **66**, 899 (1994).

⁴S. Goedecker, Rev. Mod. Phys. **71**, 1085 (1999).

⁵A. Shukla, M. Dolg, and H. Stoll, Chem. Phys. Lett. **294**, 126 (1998); A. Shukla, M. Dolg, P. Fulde, and H. Stoll, Phys. Rev. B **57**, 1471 (1998).

⁶N. Marzari and D. Vanderbilt, Phys. Rev. B **56**, 12 847 (1997); P.L. Silvestrelli, N. Marzari, D. Vanderbilt, and M. Parrinello, Solid State Commun. **107**, 7 (1998).

⁷S. Satpathy and Z. Pawłowska, Phys. Status Solidi B **145**, 555 (1988); B. Sporkmann and H. Bross, Phys. Rev. B **49**, 10 869 (1994).

⁸M.R. Pederson and C.C. Lin, Phys. Rev. B **35**, 2273 (1987); P. Fernández, A. Dal Corso, A. Baldereschi, and F. Mauri, *ibid.* **55**, R1909 (1997).

⁹U. Stephan and D.A. Drabold, Phys. Rev. B **57**, 6391 (1998).

¹⁰W. Kohn, Phys. Rev. **115**, 809 (1959); E.I. Blount, in *Solid State Physics*, edited by F. Seitz and C. Turnbull (Academic, New York, 1962), Vol. 13, p. 305, esp. Appendix C.

¹¹J. Des Cloizeaux, Phys. Rev. **135**, A685 (1964); **135**, A698 (1964); W. Kohn, Chem. Phys. Lett. **208**, 167 (1993); A. Nenciu and G. Nenciu, Phys. Rev. B **47**, 10 112 (1993).

¹²S. Ismail-Beigi and T. Arias, Phys. Rev. Lett. **82**, 2127 (1999).

¹³R. Baer and M. Head-Gordon, Phys. Rev. Lett. **79**, 3962 (1997).

¹⁴W. Kohn and J.R. Onffroy, Phys. Rev. B **8**, 2485 (1973); J.J. Rehr and W. Kohn, *ibid.* **10**, 448 (1974).

¹⁵For this reason, we argue that simple derivations of the gap dependence of WF's or the density matrix based on the HOMO-LUMO gap (cf. Ref. 13) cannot be correct in general.

¹⁶B.R. Djordjevic, M.F. Thorpe, and F. Wooten, Phys. Rev. B **52**, 5685 (1995).

¹⁷S. Goedecker and M. Teter, Phys. Rev. B **51**, 9455 (1995); R. Baer and M. Head-Gordon, J. Chem. Phys. **107**, 10 003 (1997).

¹⁸O.F. Sankey and D.J. Niklewski, Phys. Rev. B **40**, 3979 (1989).

¹⁹U. Stephan, D.A. Drabold, and R.M. Martin, Phys. Rev. B **58**, 13 472 (1998).

²⁰W. Kohn, Phys. Rev. B **7**, 4388 (1973).

²¹V. Heine, D.W. Bullett, R. Haydock, and M.J. Kelly, in *Solid State Physics*, edited by F. Seitz, C. Turnbull, and H. Ehrenreich (Academic, New York, 1980), Vol. 35.

²²P.W. Anderson, Phys. Rev. Lett. **21**, 13 (1968).

²³J. Dong and D.A. Drabold, Phys. Rev. Lett. **80**, 1928 (1998).

²⁴F. Mauri and G. Galli, Phys. Rev. B **50**, 4316 (1994); P. Ordejón, D.A. Drabold, R.M. Martin, and M.P. Grumbach, *ibid.* **51**, 1456 (1995).